Oxygen Transport in Hollow Fiber Membrane Bioreactors for 3D Cell Culture

Group 3

Sikandar Batra (sikandab)
Matthew Chin (mgchin)
Jingxuan Li (jingxual)
Rui Yao (ruiyao)

Table of Contents

Abstract **3**

Introduction **4**

Geometric Setup **5**

Mathematical Modeling **6**
- Assumptions 6
- Governing Equations 7
- Parametric Sweeps 9
- Meshing 10

Results & Discussion **11**
- Mesh Independent Study 12
- Baseline 13
- Membrane Porosity Sweep 18
- Inner Fiber Diameter (Membrane Thickness) Sweep 20
- Unit Cell Height Sweep 22

Conclusion **24**

References **26**

Abstract

In this paper, we build upon the work of Khakpour et al. for culturing cells in a hollow fiber bioreactor.[1] For this experiment, a crossed orientation is used with half the fibers supplying an oxygenated medium and the rest removing it. Hepatocytes are seeded in spheroids within unit cells of the 3D scaffold. The unit cell geometry is defined by the dimensions 750 x 750 x 500 μm (L x W x H). We assume fully developed laminar flow defined by an average velocity within the lumens. Convective mass transfer of oxygen occurs in the lumens. Diffusive mass transfer then delivers it through the porous membrane, the extra-capillary space, and into the porous spheroid. Tortuosity of the porous regions is determined through correlations developed by Bruggeman and Wako-Smith.[1] The entire system is isothermal and operating under steady state conditions. The lumen inlets have a constant concentration equal to the saturated oxygen concentration in the medium. Our model has all the fibers inflowing oxygen to improve the objective, the spheroid surface concentration and the oxygen transfer to the spheroid. Oxygen consumption within the spheroid is modeled by Michaelis-Menten kinetics.

We start the simulation by modeling the oxygen concentration in the bioreactor with the baseline dimensions and parameters using COMSOL. As an extension to the paper, we conduct parametric sweeps on the following parameters: membrane porosity, membrane thickness, and unit cell height. We use these to judge the feasibility of achieving high oxygen concentrations at the surface of and within the spheroids. Our results indicate that the oxygen concentration profile at the spheroid surface is strongly affected by the membrane porosity and inner fiber diameter. The unit cell height has a minimal effect on concentration. None of the sweeps demonstrated significant changes in the proportion of cells within the spheroid, set at a constant volume, observing a nonzero concentration.

Introduction

In this project, we build upon the work of Khakpour et al. for the growth of a cell culture in a 3D hollow fiber membrane bioreactor (HFMBR).[1] Here, the HFMBR is primarily utilized in the development of liver tissue constructs that are subsequently applied in the field as bioartificial livers or as in vitro models for drug testing and development. For simulation purposes, we model a unit cell within a 3D rectangular mesh-like scaffold with a spheroid of hepatocytes seeded at the center. We set all the fibers to inflow dissolved oxygen to the system. Diffusion transfers such to the spheroid which uptakes it through Michaelis-Menten kinetics. Our goal is to perform various parametric sweeps on the membrane properties (porosity and thickness) and unit cell dimensions (height) to observe their effects on our objective, the oxygen concentration at the spheroid surface.

The HFMBR is a type of bioreactor prized for its high surface area, a feature well-suited for improving molecule transfer to cultured cells. The system uses hollow fibers, which are thin, semi-permeable capillary membranes, usually arranged in a parallel array in a singular direction. They are generally made from a porous polymer. In our case, this is polysulfone. These hollow fiber membranes are bundled within a housing to create the HFMBR. The reactor has two domains: the fibers and the extra-capillary space. The fibers also have two domains: the hollow lumen where fluid flows and the membrane.

Inside the fibers, the flowing fluid supplies and removes the medium containing dissolved oxygen, nutrients, growth factors, waste, etc. Utilizing the diffusion process to cross the membranes, small molecules, including simple sugars or drugs, can freely diffuse while large eukaryotic cells cannot. Outside the fibers, cells are separated from the flowing medium by the membrane. There are various seeding methods, with the simplest being injection, to spread the cells throughout the extra-capillary space. Note that there are some rare setups which place the cells in the lumens and flow the medium in the extra-capillary space.

HFMBRs have several advantages.[1] First, as stated earlier, is the tremendous amount of surface area in a small volume enabling cells to grow on and around the fibers at high densities. Second is the potential enhancement of mass transfer rates by improving the concentration gradients. Third is protection of the cells against shear stress due to their placement within the extra-capillary space.

Khakpour et al. have developed a type of HFMBR utilizing a 3D crossed array of fibers. There are two orientations of parallel arrays of fibers versus the usual one. This forms a 3D rectangular mesh-like structure that serves as scaffolding for the seeded cells. In tissue engineering, the three core components needed for proper tissue growth are scaffolding, nutrients, and growth factors. This unique HFMBR orientation provides all and allows for tissue cultivation if run for longer periods of time. However, our simulation focuses on shorter time scales with the spheroid volume being constant.

Unfortunately, this crossed structure slightly works against the large surface area benefit

provided by normal HFMBRs. Since cells are clumped into spheroids and not dispersed throughout the extra-capillary space, the interior cells cannot take full advantage of the enhanced mass transfer. In short, a lower proportion of cells are in direct contact with a fiber than in a normal HFMBR setup.

In this system, the geometry is unique for innovative crossed fibers packed within each unit cell. Different from most normal HFMBR setups with unidirectional flow, this system has flow in two directions. In the paper, oxygenated growth medium flows through half the fibers oriented in one direction. The other half removes growth medium and any wastes from the extra-capillary space. Our setup involves inflowing an oxygenated medium within all the fibers to improve oxygen delivery to the spheroid.

In this project, our goal is to perform various parametric sweeps on the membrane properties and unit cell dimensions. We also calculate the dimensionless Peclet number (*Pe*) for the extra-capillary space and the dimensionless Damkohler number (*Da*). These values allow us to determine the rate limiting steps within mass transfer or between mass transfer and oxygen consumption.

Geometric Setup

As shown below in **Figure 1**, the overall shape of a unit cell element within a crossed HFMBR is a 3D rectangular scaffold with the dimensions 750 × 750 × 500 μm (*L* × *W* × *H*). The spheroid of hepatocytes is trapped in the center of the unit cell formed by the crossed fibers. Parallel fibers are 250 μm apart, also known as the inter-hollow-fiber spacing. The fluid in the top two fibers flows along the positive y-direction while the fluid in the bottom two flows in the positive x-direction. The diameter of the fiber is 250 μm while the inner diameter is 150 μm. This results in the crossed fibers touching each other at singular points. The spheroid has a diameter of 300 μm.

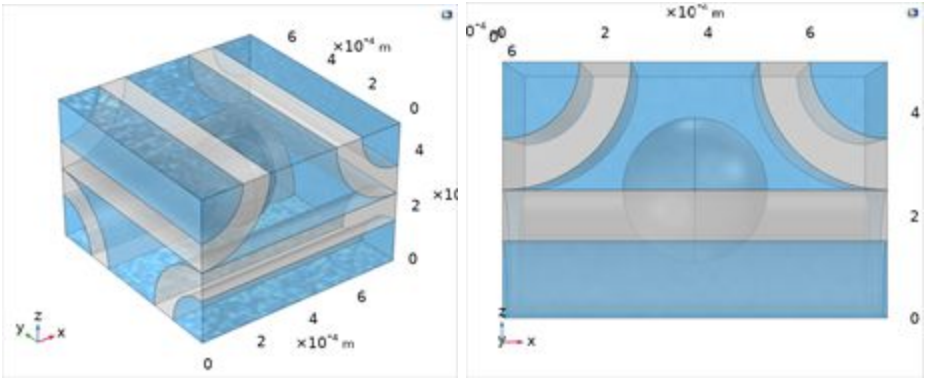

Figure 1: (Left) unit cell; (right) xz-plane of the unit cell. Blue domains are fluid while the others are solid.

Mathematical Modeling

In this section, we discuss the mathematical models used in our simulation. These are described as physics modules in COMSOL.

Assumptions

Our model contains several assumptions. The first set is that flow within the lumens can be described by fully developed laminar flow with an average velocity, and the concentration at the inlet to each lumen is defined by a constant concentration across the cross section described by the saturated oxygen concentration in the medium. The value we used for all our simulations is the baseline value from Khakpour et al. of 185 μmol/L.[1] Another important assumption is setting the growth medium as water. Biological growth medium used for in vitro studies usually contain nutrients such as agar and any growth factors needed to induce stem cell differentiation. However, since these components only represent a small portion of what is mainly a water-based solution, we assume the entirety of the medium to be water. This means that we assume the viscosity, density, and diffusivity of oxygen in the medium is not heavily influenced by the additional components. In addition, the use of water as the medium means that the fluid is incompressible.

Returning to the assumption of constant concentration at the inlets, this implies that the outlet concentration of the adjacent unit cell is also constant. However, since we made the assumption of a fully developed laminar flow in the lumens, the result is that the concentration throughout the lumen is relatively equal to that of the inlet, thus satisfying this implication. The paper demonstrated similar results for the two bottom lumens within the unit cell inflowing oxygen.[1]

Other various assumptions include the fact that the system is isothermal and at steady state, thus allowing us to use stationary studies in COMSOL.

One final assumption we make is that the spheroid size, namely the diameter, remains constant. To reiterate, the primary purpose of our project is to study and optimize the parameters affecting the surface concentration of oxygen at the spheroid. This is because there are far more of these parameters that can be readily changed in an experiment. Due to the specific method used to seed and pack the spheroids within the unit cells, the initial porosity and density are not easily changed.[1] Diameter is the only main spheroid parameter that can be swept for. Since we use a constant value for the maximum oxygen uptake rate, V_{max}, it is logical that as the cells grow and the spheroid diameter increases, the proportion of cells within the spheroid observing a low oxygen concentration will also increase. However, since our goal is to ensure sufficient oxygen delivery to the spheroid surface, we believe that our optimized parameters providing maximum

surface concentration will be sufficient to account for spheroid expansion in experimental studies from the baseline diameter of 300 μm.

Governing Equations

The velocity profile in the lumens is defined by a simple fully developed laminar flow. In these free flow regions, the oxygen mass transfer is coupled to hydrodynamics. In other words, convective mass transfer dominates within the lumens. To model said physics, dilute species transport was utilized. The conservation equation that characterizes the free fluid regions is given by **Equation 1** below.

To model the porous media regions, i.e. membranes and spheroid, the effective diffusivity and oxygen consumption terms are added to the prior equation. It should be noted that the oxygen consumption term is only nonzero within the spheroid. The conservation equation that characterizes the porous media regions is given by **Equation 2** below.

$$\cdot (c_{ox,i}\bar{u}_i) - \cdot (D_{ox,i}c_{ox,i}) = 0 \qquad \textbf{[Equation 1]}$$

$$\cdot (c_{ox,i}\bar{u}_i) - \cdot (D_{e_{ox,i}}c_{ox,i}) - R_o = 0 \qquad \textbf{[Equation 2]}$$

Inlet boundary conditions of the lumens include fully developed laminar flow with an average velocity of 2.4E-3 m/s and constant concentration at the saturated oxygen concentration of 185 μmol/L. Outlet boundary conditions of the lumens include the same average velocity as the inlet and zero normal concentration gradient. Lumen unit cell surfaces that are not an inlet or outlet are described by symmetry. Membrane unit cell surfaces perpendicular to the respective inlet are described by symmetry. Extra-capillary space unit cell surfaces and remaining membrane unit cell surfaces are described by periodic boundary conditions.

Constitutive Laws

The metabolic rate of oxygen consumption is modelled by Michaelis-Menten kinetics shown below in **Equation 3**. V_{max} is the maximum consumption rate. K_M is the concentration at which $\frac{V_{max}}{2}$ is reached.

$$R_{mm} = \frac{V_{max}\, c_{ox,cc}}{c_{ox,cc} + K_m} \qquad \textbf{[Equation 3]}$$

The effective diffusion coefficient of oxygen ($D_{e_{ox,i}}$) in the porous media regions is given by **Equation 4** below. The diffusion coefficient oxygen in any domain ($D_{ox,i}$) is a predetermined value. Values for the various domains are given in **Table 1** below. ε_i is the porosity of the porous domain *i*. τ_i is the tortuosity of porous domain *i*. The Bruggeman equation, **Equation 5**, is used to determine the tortuosity of the spheroid, or cellular compartment, while the

Wakao-Smith equation, **Equation 6**, is used to determine the tortuosity of the membrane.

$$D_{e_{ox,i}} = \frac{\varepsilon_i}{\tau_i} D_{ox,i} \qquad \textbf{[Equation 4]}$$

$$\tau_{cc} = \frac{1}{\varepsilon_{cc}^{0.5}} \qquad \textbf{[Equation 5]}$$

$$\tau_m = \frac{1}{\varepsilon_m} \qquad \textbf{[Equation 6]}$$

Table 1: Parameter Baseline Values

Parameter	Description	Baseline Value	Units
Bioreactor Parameters			
δ_{HF}	inter-hollow-fibre spacing between parallel fibers	150	μm
l_{lmnt}	characteristic length		μm
ε_m	porosity of membrane	0.7	
τ_i	tortuosity of porous domain *i*		
l_{lmnt}	characteristic length		μm
Fluid Parameters			
T	temperature	310.15	K
ρ_f	fluid density	997	kg/m^3
μ_f	fluid dynamic viscosity	0.0006922	kg/m/s
u_i	fluid velocity (vector field) in domain *i*		m/s
p_i	pressure in domain *i*		Pa
U_{avg}	mean luminal velocity	2.4E-3	m/s
$c_{ox,i}$	oxygen concentration in domain *i*		μmol/L
$c_{ox,sat}$	saturated oxygen concentration in equilibrium with the oxygen partial pressure in the gas phase	185	μmol/L
$D_{ox,water}$	diffusivity of oxygen in water	3.4E-9	m^2/s
$D_{ox,m}$	diffusivity of oxygen in membrane	3.4E-10	m^2/s
$D_{ox,cc}$	diffusivity of oxygen in spheroid	3.4E-9	m^2/s
Cell Parameters			
d_{sph}	spheroid diameter	300	μm
d_{hep}	mean diameter of hepatocytes	16	μm
ε_{cc}	porosity of spheroid	0.2	
R_{MM}	oxygen consumption rate		mol/m^3/s

$\mathbf{V_{max}}$	maximum consumption rate in Michaelis-Menten kinetics	5	nmol/cm^3/s
$\mathbf{K_M}$	concentration at which the oxygen uptake rate is half V_{max}	7.8	μmol/L

Numerical Methodology

The goal of our project is to optimize the mass transfer of oxygen to the spheroid. Thus, the main result we analyze for all our simulations is the spheroid surface concentration of oxygen. A higher value usually indicates higher steady state mass transfer from the lumens to the spheroid at a constant spheroid size and oxygen consumption rate. Since the spheroid parameters are a function of the specific seeding technique and cells used, we concentrate on varying the HFMBR parameters while leaving the spheroid parameters at the baseline values given by Khakpour et al. for hepatocytes forming a spheroid with a diameter of 300 μm and maximum oxygen consumption rate, V_{max}, of 5 nmol/s/cm^3 and a Michaelis constant, K_M, of 7.8 μmol/L. Note that temperature in all domains is constant at 310.15 K, spheroid porosity is constant at 0.2, diffusivity of oxygen in water used as a baseline value is 3.4E-9 m^2/s, and saturated oxygen concentration is constant at 185 μmol/L. The baseline membrane porosity is 0.7, the baseline inner fiber diameter is 150 μm, and the baseline unit cell height is 500 μm.

Parametric Sweeps

The parameters we sweep include membrane porosity, membrane thickness with the total fiber diameter value being constant at the baseline of 250 μm, and height (z-axis) of the unit cell to increase the vertical spacing between the crossed fibers.

For membrane porosity, we test the values 0.2, 0.32, 0.44, 0.56, 0.68, and 0.8. We expect the surface oxygen concentration of and the mass transfer of oxygen to the spheroid to increase with increasing membrane porosity due to lower resistance along the path from the lumen to the spheroid. Since the fiber sizes do not change, we first run a study using just the laminar flow physics to calculate the velocity and pressure profiles within the lumens. Then we run a parametric sweep study using just the dilute mass transfer in porous media physics to calculate the concentration profile throughout the entire geometry using the solution from the laminar flow study for the convective mass transfer in the lumens. We use the default stationary solver settings for the laminar flow study, which is acceptable due to the simplicity allowed by assuming a fully developed laminar flow with a specified average velocity of 2.4E-3 m/s at the inlet of the lumens. For the parametric sweep, we used the stationary solver with parametric, segregated, and direct methods. Within the segregated method settings, we use the default settings of tolerance termination with a maximum iteration count of 300, a segregated step combining all variables (u,

p, and *c*), and a lower limit of zero on *c*. Within the direct method settings, we use the PARDISO solver, as this was the only solver that converged, with a pivoting perturbation of 1E-13.

For membrane thickness where we sweep the inner diameter of the fibers, we test the values 75, 105, 135, 165, 195, and 225 μm. We expect the surface oxygen concentration of and the mass transfer of oxygen to the spheroid to increase with increasing inner diameter (decreasing membrane thickness) due to lower resistance along the path from the lumen to the spheroid. Since the lumen sizes change, we first run a stationary, parametric sweep study using just the laminar flow physics with default solver settings. Then we run a parametric sweep study using just the dilute mass transfer physics in porous media physics. Here, we used the stationary solver with segregated and direct methods. Within the segregated method settings, we use the default settings with a maximum iteration count of 300, a segregated step combining all variables, and a lower limit of zero on *c*. Within the direct method settings, we use the PARDISO solver with a pivoting perturbation of 1E-13.

For unit cell height, we test the values 500, 550, 600, 650, 700, and 750 μm. The lowest value of 500 μm is the baseline height where the crossed fibers touch. As the value increases, they no longer touch. We expect the surface oxygen concentration of the spheroid to decrease with increasing unit cell height due to the increased distance from the fibers to the spheroid. Since the lumen positions change, we first run a stationary, parametric sweep study using just the laminar flow physics with default solver settings. Then we run a parametric sweep study using just the dilute mass transfer physics in porous media physics. Here, we used the stationary solver with segregated and direct methods. Within the segregated method settings, we use the default settings with a maximum iteration count of 500, a segregated step combining all variables, and a lower limit of zero on *c*. Within the direct method settings, we use the PARDISO solver with a pivoting perturbation of 1E-13.

Meshing

Our mesh, shown for the unit cell's surfaces in **Figure 2** below, consists of using free tetrahedral elements across all domains with the default settings. At the inner membrane, outer membrane, and spheroid surface boundaries, we specify two boundary layers with the rest of the settings at default. Our main way of controlling the mesh quality is by changing the element size within each domain. As ours results later show, this is adequate for determining the objectives of the project. However, it should be noted that when the crossed fibers touch when the unit cell height is 500 μm, the pinch point where the crossed fibers meet has lower accuracy at and around it due to the minimum element size near this feature being larger than the feature itself. However, the concentration profile near these features is not within the scope of the project's objective and does not significantly affect it, if at all.

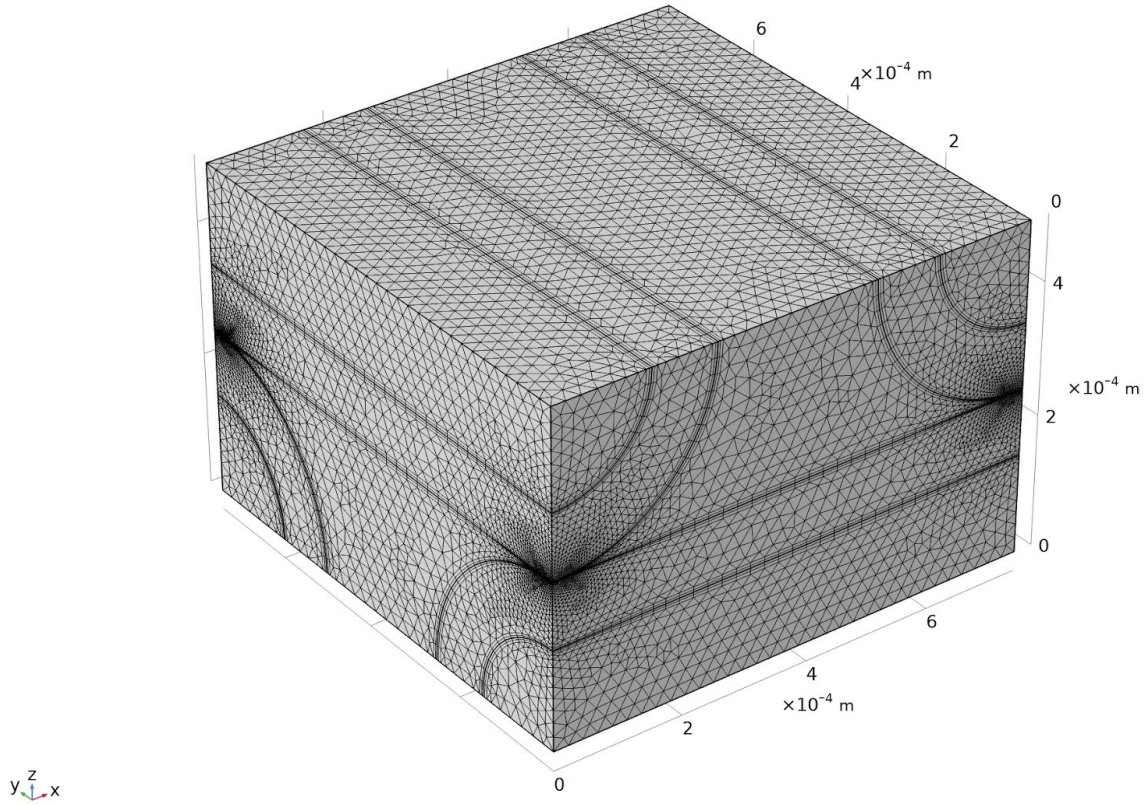

Figure 2: Unit cell surface mesh. Minimum element size is "finer" or 2.45E-6 m.

Results & Discussion

In this section, we provide and analyze the results from our simulations. Some important dimensionless numbers relevant to our model are the Peclet number (*Pe*) for the extra-capillary space and the Damkohler number (*Da*). The Peclet number, calculated in **Equation 9** below, is a ratio of the convective to diffusive mass transfer rates. The term l_{lmnt} here is the length of a lumen within the unit cell where convective mass transfer occurs. For our simulations, this number is very large which indicates that the diffusive mass transfer through the extra-capillary space (and membrane) is rate limiting. The Damkohler number, calculated in **Equation 10** below, is a ratio of the oxygen consumption to the external (to the spheroid) diffusion rates. The term l_{lmnt} here is the length between parallel fibers, known as the inter-hollow-fiber spacing. For our simulations, this number is slightly below 1 which indicates that the oxygen consumption rate is slightly rate limiting and could result in a small buildup of oxygen at the outer spheroid layers. In other words, the oxygen is being delivered slightly faster than it is being consumed. To meet our objective, we want this number to be at or slightly below 1, which it is.

$$Pe_{ecs} = \frac{U_{avg}\, l_{lmnt}}{D_{ox,ecs}} = \frac{(2.4{*}10^{-3}\ m/s)\,(750{*}10^{-6}\ m)}{(3.4{*}10^{-9}\ m^2/s)} = 529 \qquad \textbf{[Equation 9]}$$

$$Da = \frac{V_{max}\,(l_{lmnt})^2}{D_{ox,ecs}\,C_{ox,sat}} = \frac{(5\ \mu mol/s/L)\,(250{*}10^{-6}\ m)^2}{(3.4{*}10^{-9}\ m^2/s)\,(185\ \mu mol/L)} = 0.497 \qquad \textbf{[Equation 10]}$$

Mesh Independent Study

For the mesh independent study, we change the minimum and maximum element sizes for the domains. The values we test correspond to COMSOL's predefined element sizes of coarser, coarse, normal, fine, finer, and extra fine. The maximum element sizes include 7.96E-5, 6.12E-5, 4.1E-5, 3.25E-5, 2.27E-5, and 1.41E-5 m, respectively. The minimum element sizes include 2.45E-5, 1.84E-5, 1.22E-5, 6.12E-6, 2.45E-6, and 9.19E-7 m, respectively. These two parameters are linked in specified combinations with the first maximum element size only tested with the first minimum element size, the second maximum only tested with the second minimum, etc. **Figure 3** below displays the results.

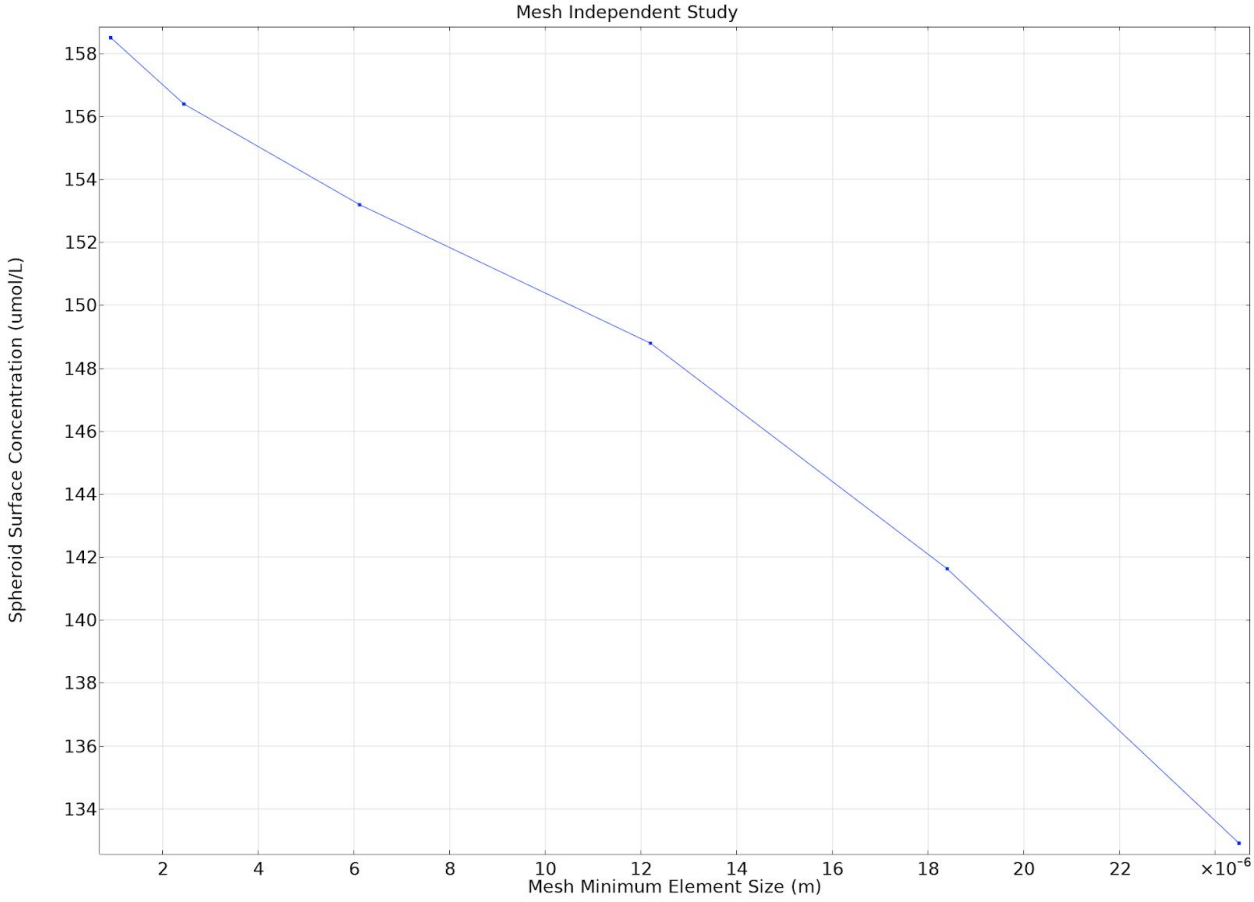

Figure 3: Mesh independent study. A lower minimum element size corresponds to a finer mesh.

As expected, a finer mesh with a smaller minimum element size (and maximum element size) yields a more accurate objective value. However, the calculation time going from “finer” to “extra fine” exponentially increases while still being within 1.3% of the most accurate value. Thus, we run all our parametric sweeps with the maximum and minimum element sizes at the default values for the “finer” preset.

Baseline

Using the baseline values described in the Mathematical Modeling section and the introduction of the Numerical Methodology section, we obtain the results shown in **Figure 4**, **Figure 5**, and **Figure 6** below. Execution time for the laminar flow study is 16 s while for the mass transfer study is 103 s. All execution times provided in this paper are the results from the same computer. **Figure 4** shows the velocity profile while **Figure 5** shows the pressure profile within the lumens. As expected, the velocity profile is very simple since all the lumen inlets have a boundary condition constraining the profile to fully developed laminar flow with a specific average velocity. Similarly, the pressure profile shows a nearly constant atmospheric pressure with no pressure drop. Even when sweeping the inner fiber diameter, the maximum velocity should not change, with the only difference being the increased length it takes for the velocity to reach 0 as the inner fiber diameter increases.

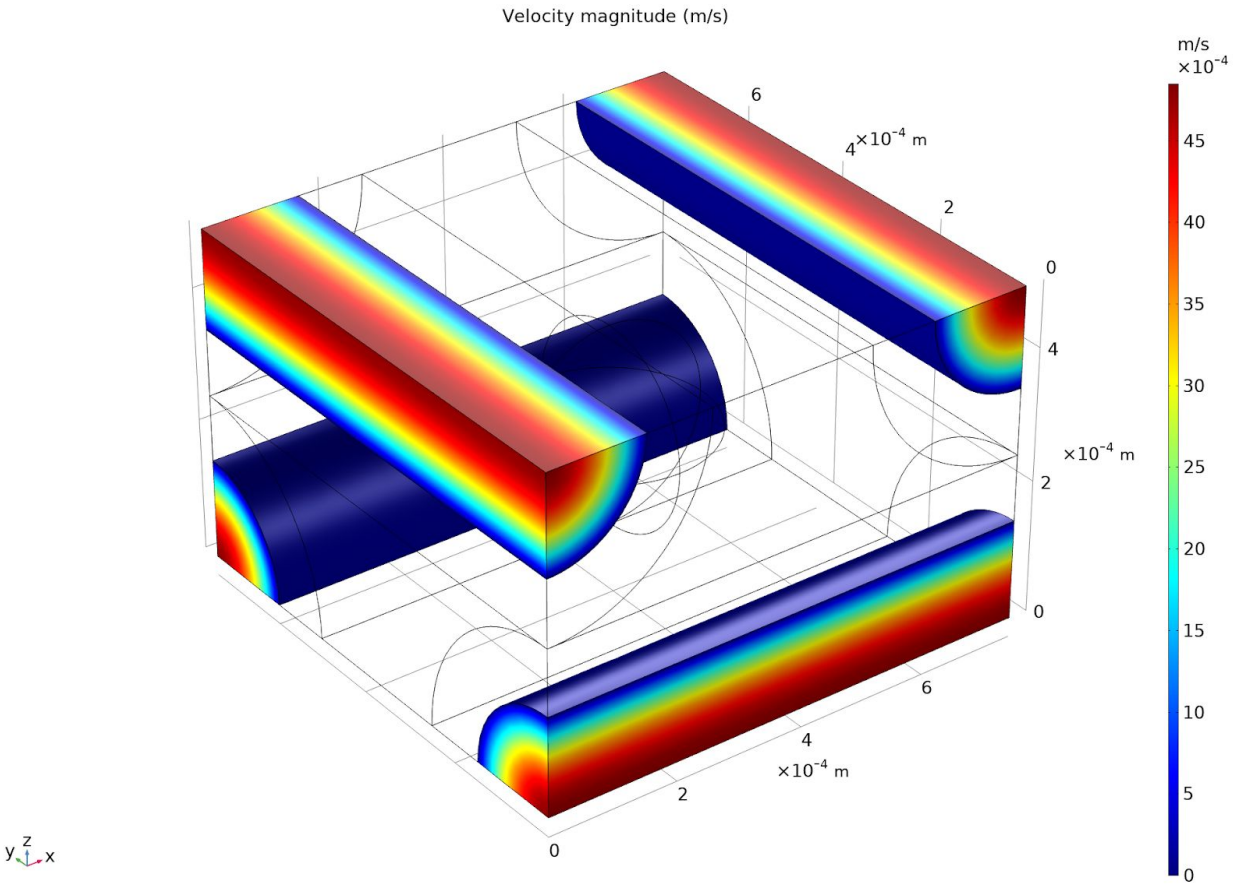

Figure 4: Lumen velocity profiles. This shows fully developed laminar flow.

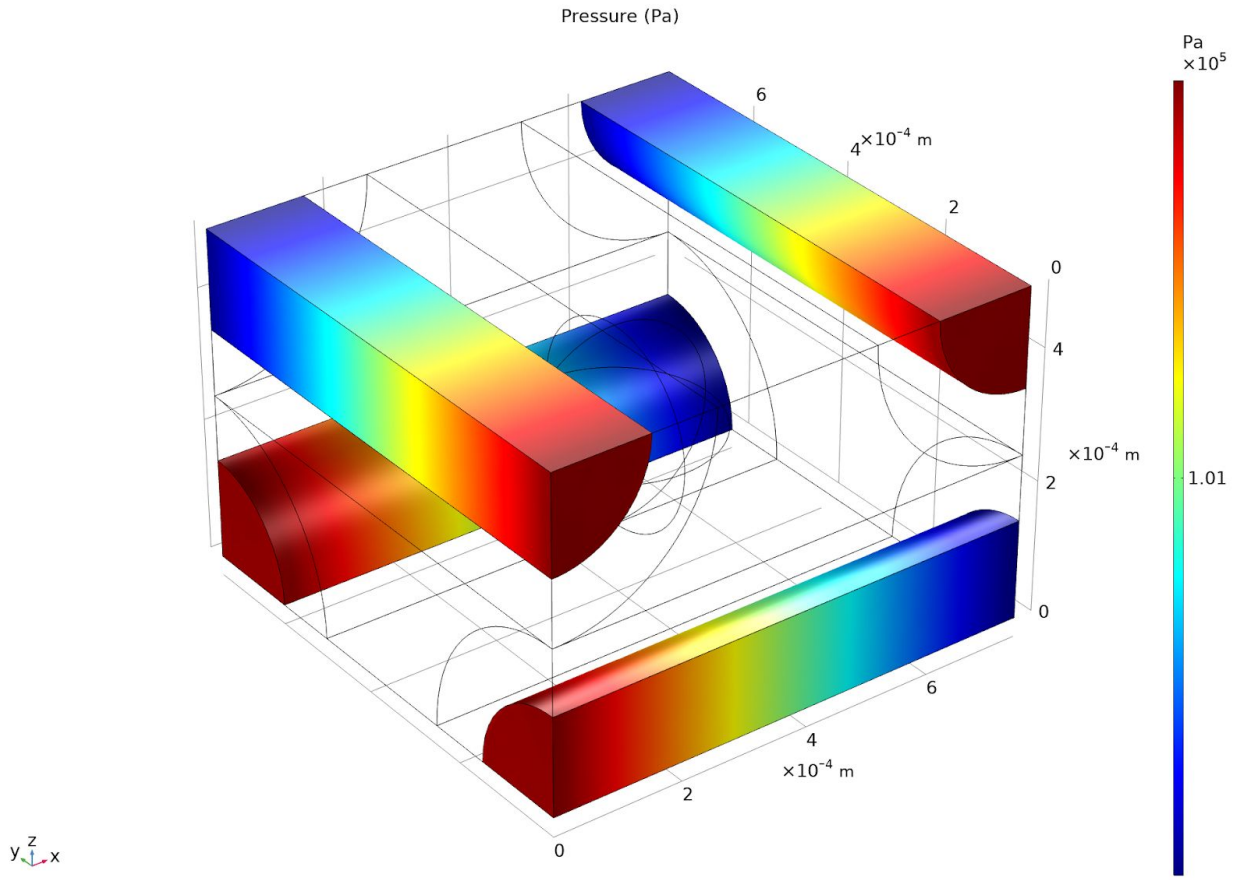

Figure 5: Lumen pressure profiles. Pressure is nearly constant.

Figure 6 below shows the concentration profile in all domains. Due to the fully developed laminar flow, the constant concentration across the inlet cross sections, and the resistance (low rate) to mass transfer out through the membrane described by the high Peclet number, the concentration within the lumens is nearly constant. Even with the membrane porosity at 0.7, the diffusivity is still on the order of 1E-10 m^2/s so at least a portion of the oxygen stays within the lumen and maintains the inlet concentration. The concentration drops moving through the membrane and into the extra-capillary space. This bulk region also experiences a relatively constant concentration. The periodic boundary conditions of the extra-capillary space's unit cell surfaces help enforce this due to mass transfer into and out of adjacent unit cells. The spheroid surface concentration is equal to that of the extra-capillary space. Note the thick outer layer with nearly the same concentration as the surface. This can be explained by the low Damkohler number since the mass transfer rate to the surface is slightly higher than the consumption rate. Past this layer, the concentration quickly drops to 0. Thus, the cells at the center are deprived of oxygen. However, it seems the proportion of cells observing a concentration of 0 is lower than that in Khakpour et al.'s setup, which only had half the fibers (bottom fibers within each unit cell) inflowing oxygen. Thus, it seems our setup with all the

fibers inflowing oxygen, while still fulfilling the other necessary roles such as inflowing nutrients and removing waste, has better oxygen delivery to the spheroid.

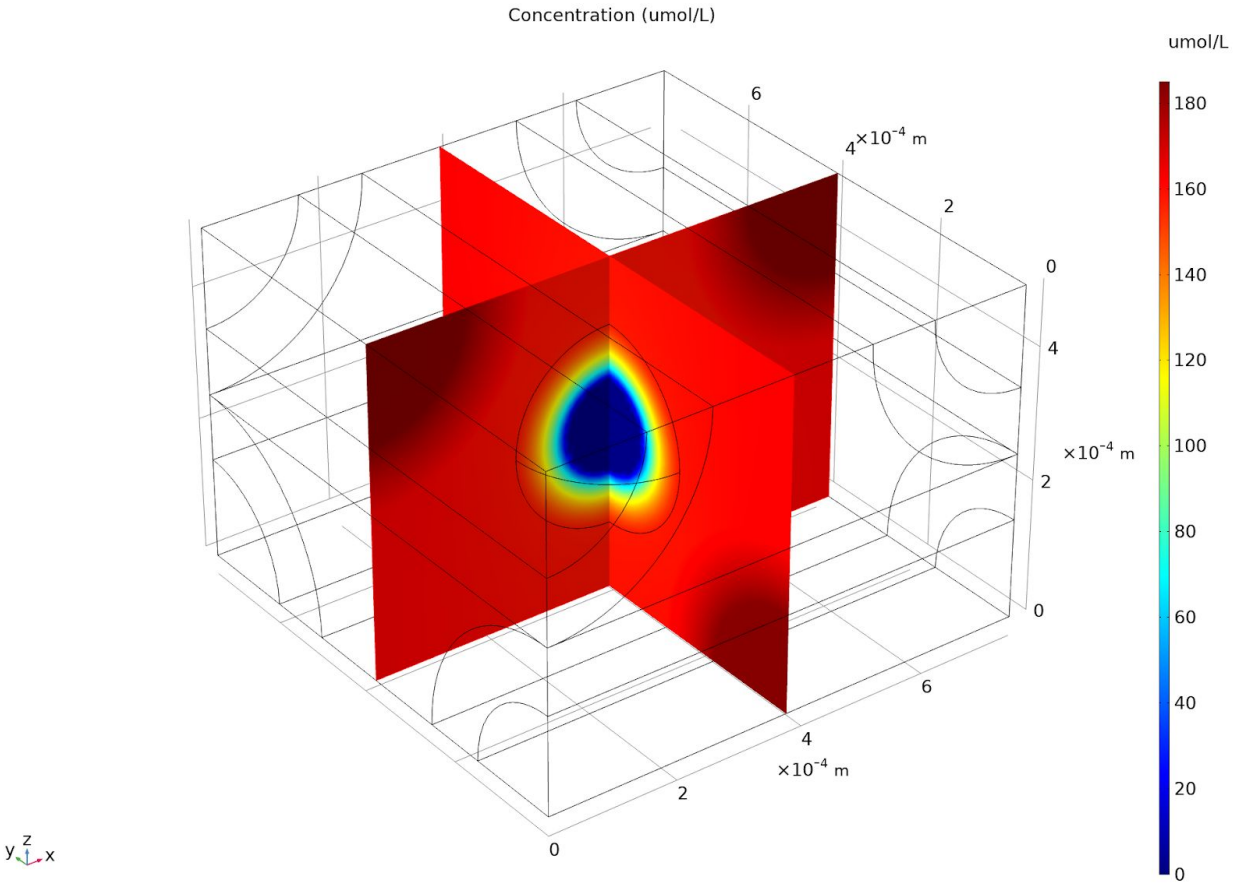

Figure 6: Concentration profile. The lumens and extra-capillary space are near constant.

Figure 7 below provides a more detailed portrayal of the concentration profile within the fibers. As seen above, the lumen concentration is constant. Once in the membrane domain, the concentration drops parabolically, with the change in concentration decreasing approaching the extra-capillary space. The final concentration is that of the extra-capillary space.

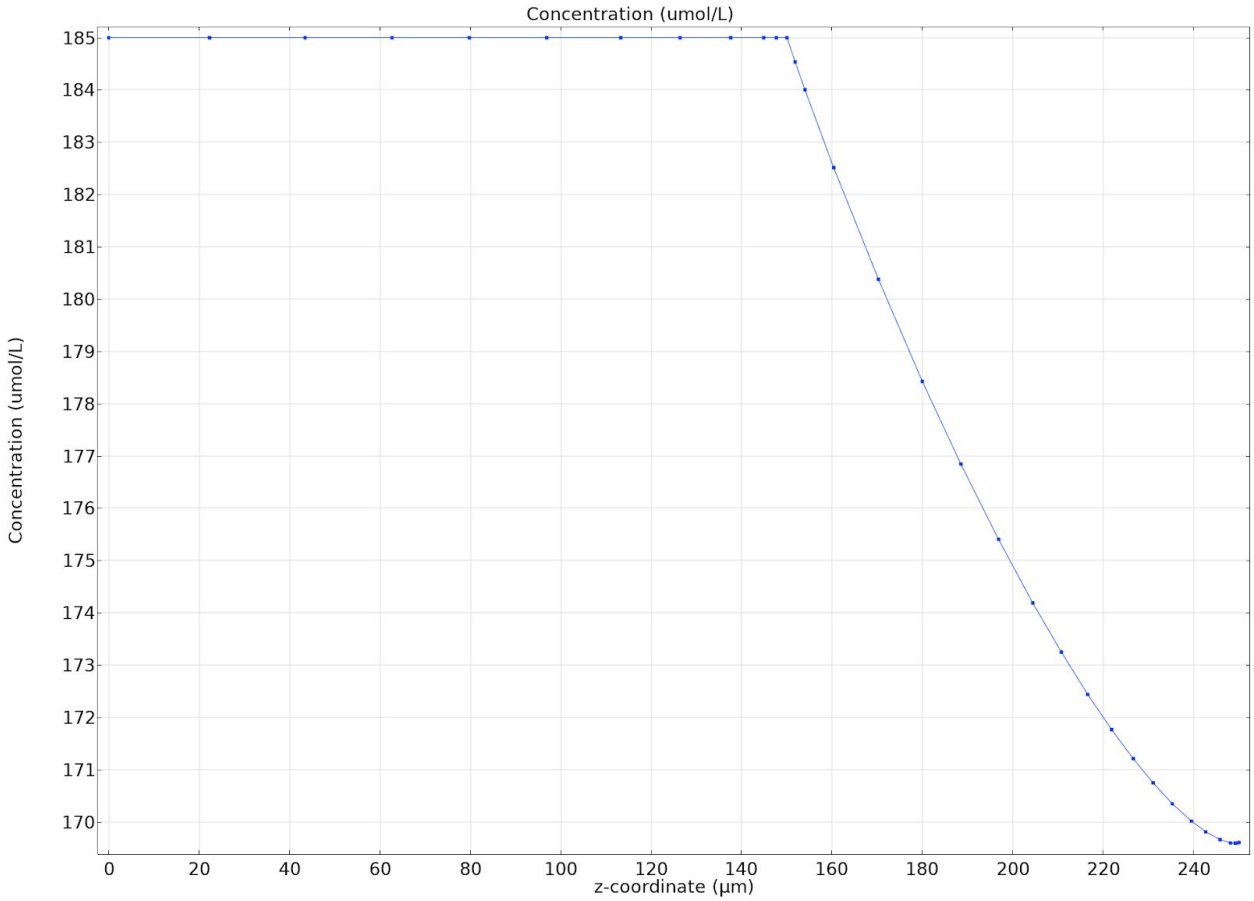

Figure 7: Fiber concentration profile. The center is at $z = 0$ while the surface is at $z = 250$.

Figure 8 below provides a more detailed portrayal of the concentration profile within the spheroid. The starting surface concentration is that of the extra-capillary space. The concentration initially drops parabolically. Near the surface, the change in concentration is low, explained by the Damkohler number being slightly below 1. Approaching half the radius, the change in concentration is high. However, as the profile further approaches the center, the concentration seems to hit an inflection point and asymptotically (but quickly) approaches 0.

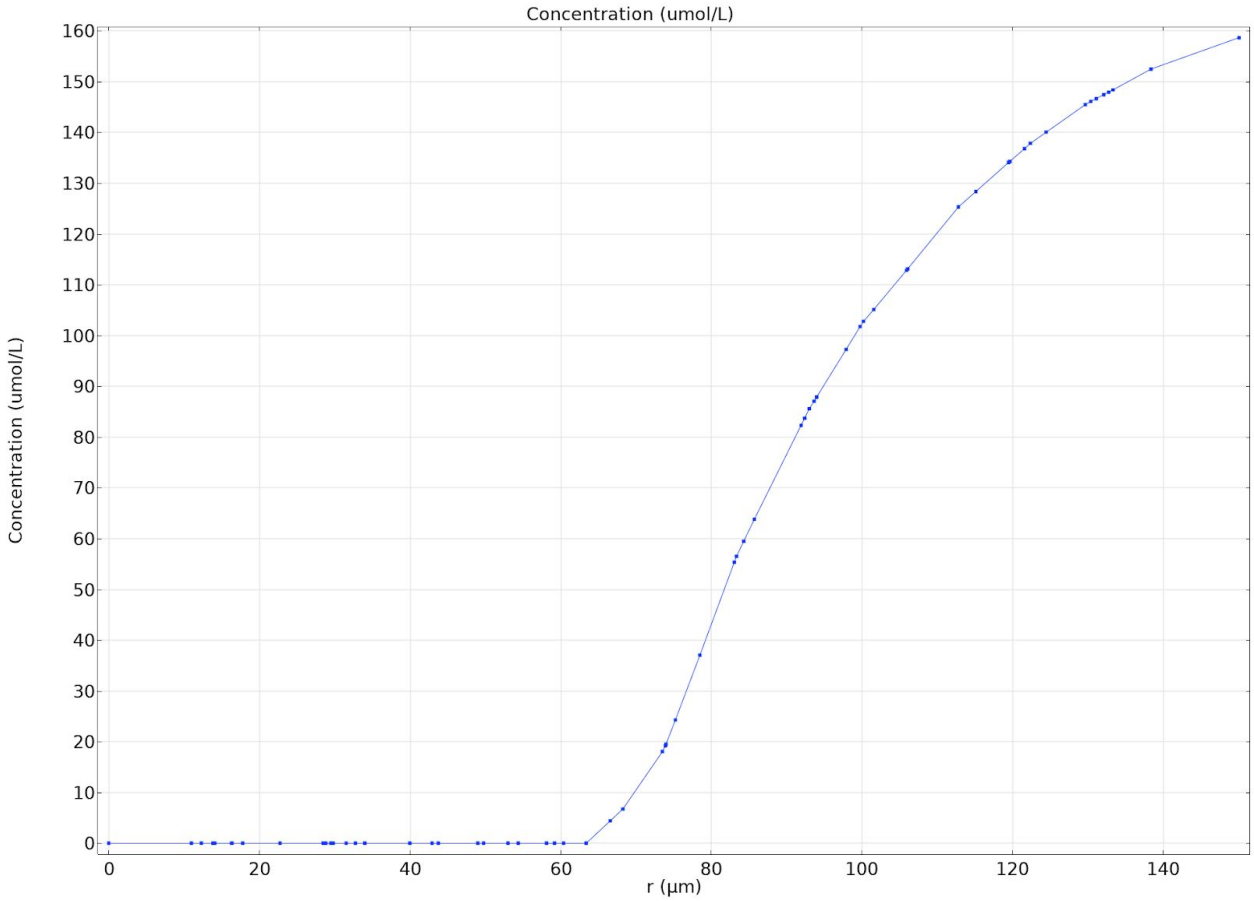

Figure 8: Spheroid concentration profile. The center is at $r = 0$ while the surface is at $r = 150$.

Membrane Porosity Sweep

In this sweep, we change the membrane porosity. Execution time for the laminar flow study is 16 s while for the mass transfer study is 55.23 min. **Figure 9** below shows the result for a porosity of 0.2. Note how the lumen concentration is the same constant value as in the baseline run. However, as the porosity decreases, the oxygen experiences more resistance diffusing through the membrane. As such, the extra-capillary space's concentration decreases as the porosity decreases. The spheroid still experiences the thick outer layer of near constant concentration equal to that of the extra-capillary space. In addition, it seems the proportion of cells observing a concentration of 0 has not changed.

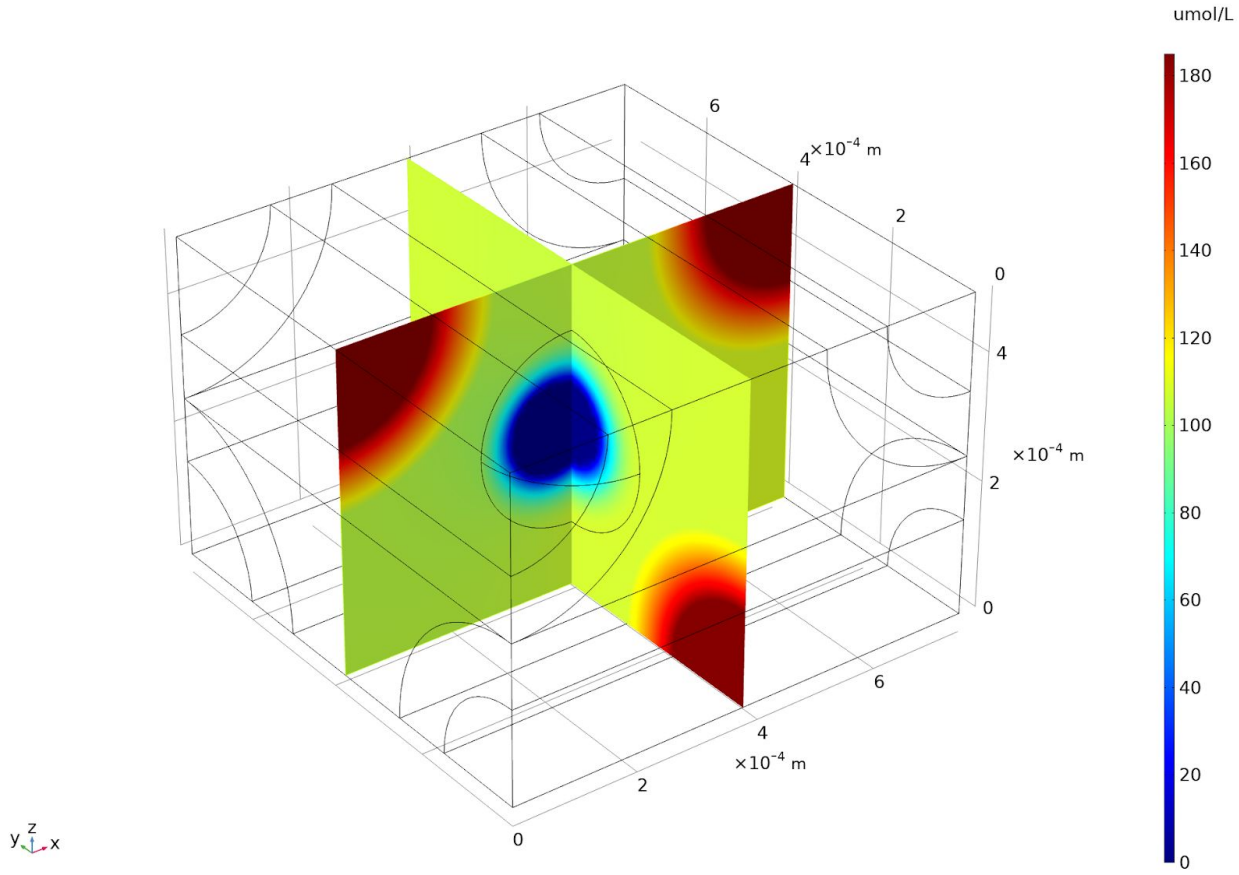

Figure 9: Concentration profile. The membrane porosity here is 0.2.

Figure 10 below shows the result of sweeping membrane porosity on the spheroid surface concentration. Increasing membrane porosity yields a parabolic increase in spheroid surface concentration. At high porosity values, increasing it any more will not yield as high of an increase in spheroid surface concentration than at low porosity values. In conclusion, a higher membrane porosity results in a higher spheroid surface concentration and better oxygen delivery.

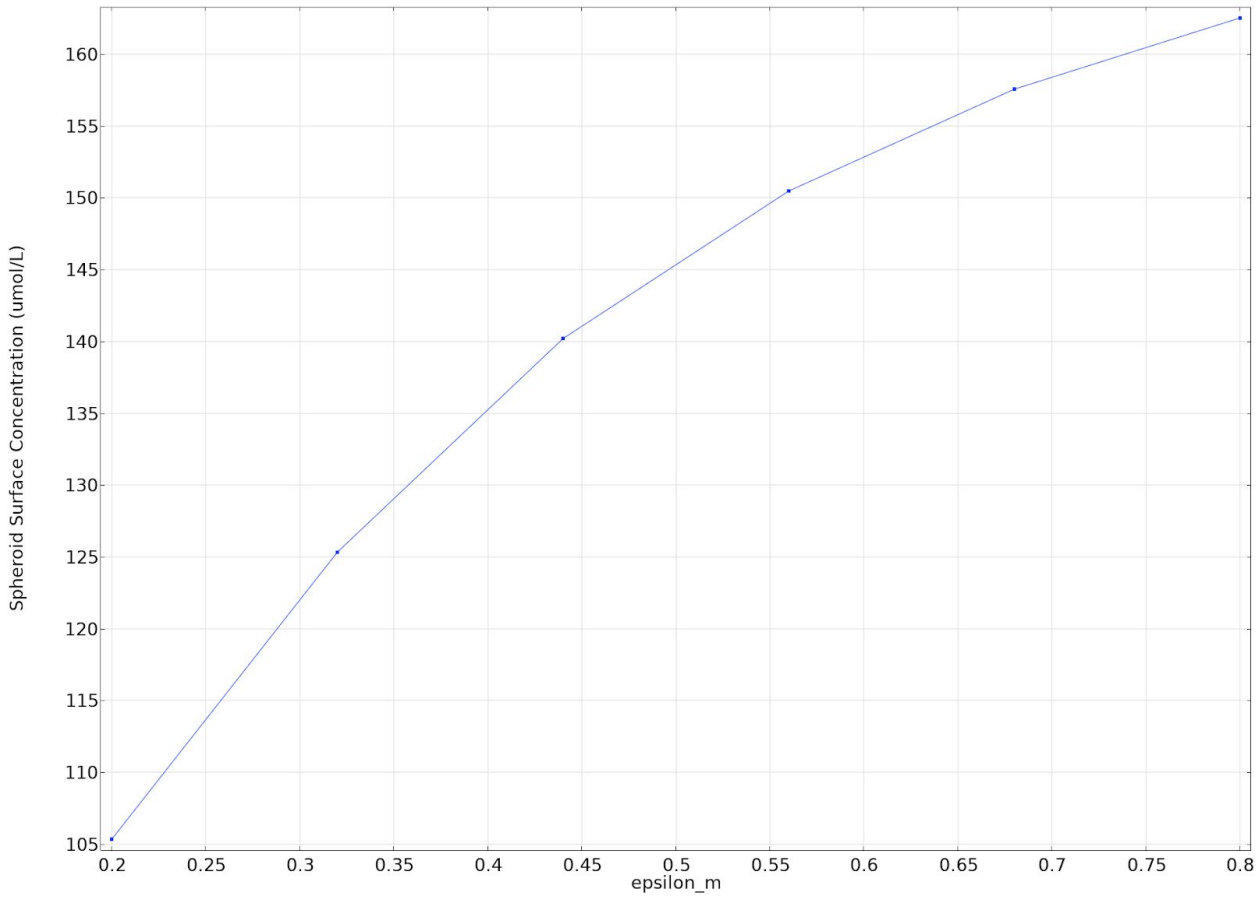

Figure 10: Spheroid surface concentration vs. membrane porosity. Higher porosity yields higher *c*.

Inner Fiber Diameter (Membrane Thickness) Sweep

In this sweep, we change the inner fiber diameter which, as a result, changes the membrane thickness while retaining the relative positions of the fibers to one another. Execution time for the laminar flow study is 8.43 min while for the mass transfer study is 36.32 min. **Figure 11** below shows the result for an inner fiber diameter of 75 μm. Note how the lumen concentration is the same constant value as in the baseline run. However, as the inner fiber diameter decreases, the membrane thickens, thus increasing the resistance the oxygen experiences along the path to the spheroid. As such, the extra-capillary space's concentration decreases as the inner fiber diameter decreases. The spheroid still experiences the thick outer layer of near constant concentration equal to that of the extra-capillary space. In addition, it seems the proportion of cells observing a concentration of 0 has not changed.

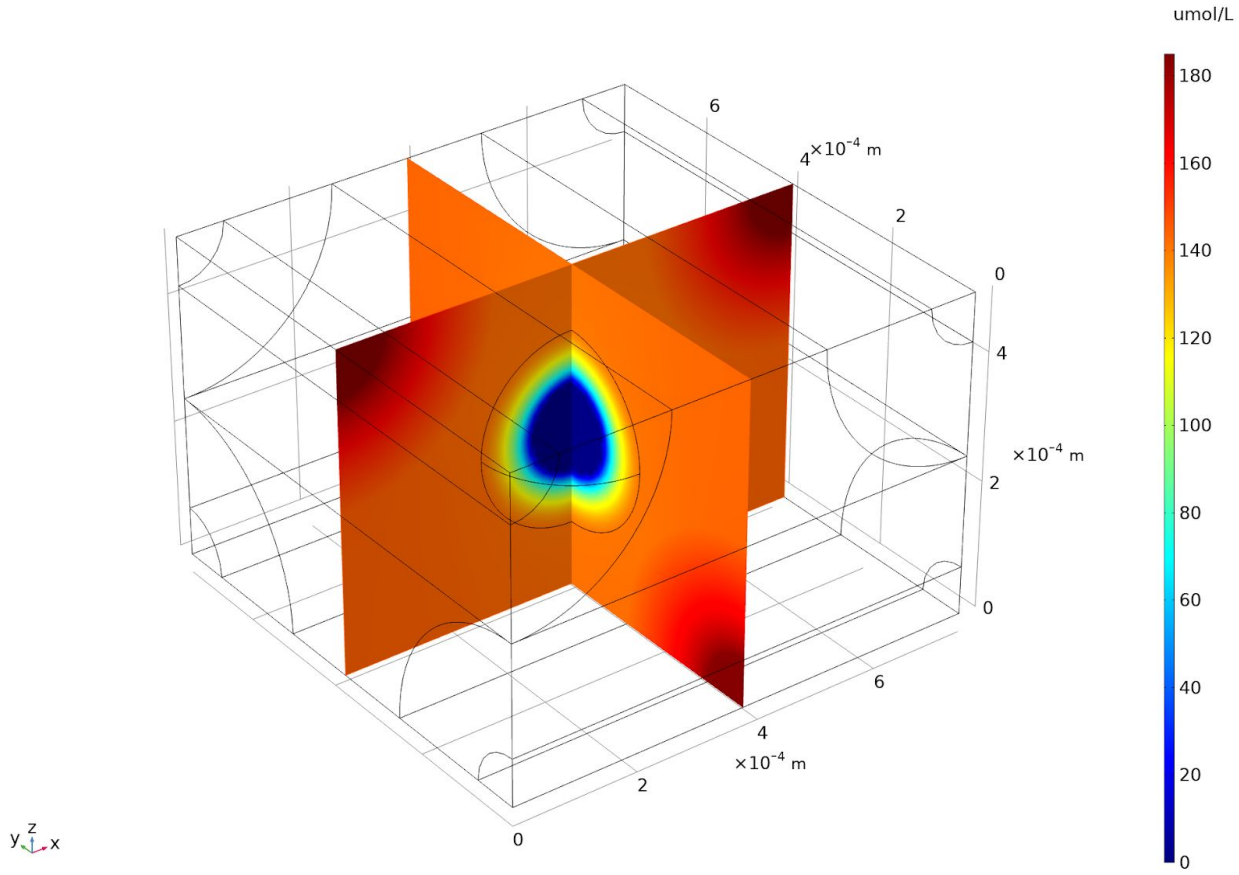

Figure 11: Concentration profile. Inner fiber diameter is 75 μm.

Figure 12 below shows the result of sweeping inner fiber diameter on the spheroid surface concentration. Increasing inner fiber diameter yields a linear increase in spheroid surface concentration. In conclusion, a larger inner fiber diameter, resulting in a thinner membrane, results in a higher spheroid surface concentration and better oxygen delivery. However, we are hesitant to recommend extreme thinning of the membranes. Doing so reduces the structural integrity of the fibers and may cause them to collapse on themselves as the spheroids grow. In addition, the shear stress of the fluid against the inner membranes may be too high at higher velocities. Structural integrity also depends on the material composition of the fibers.

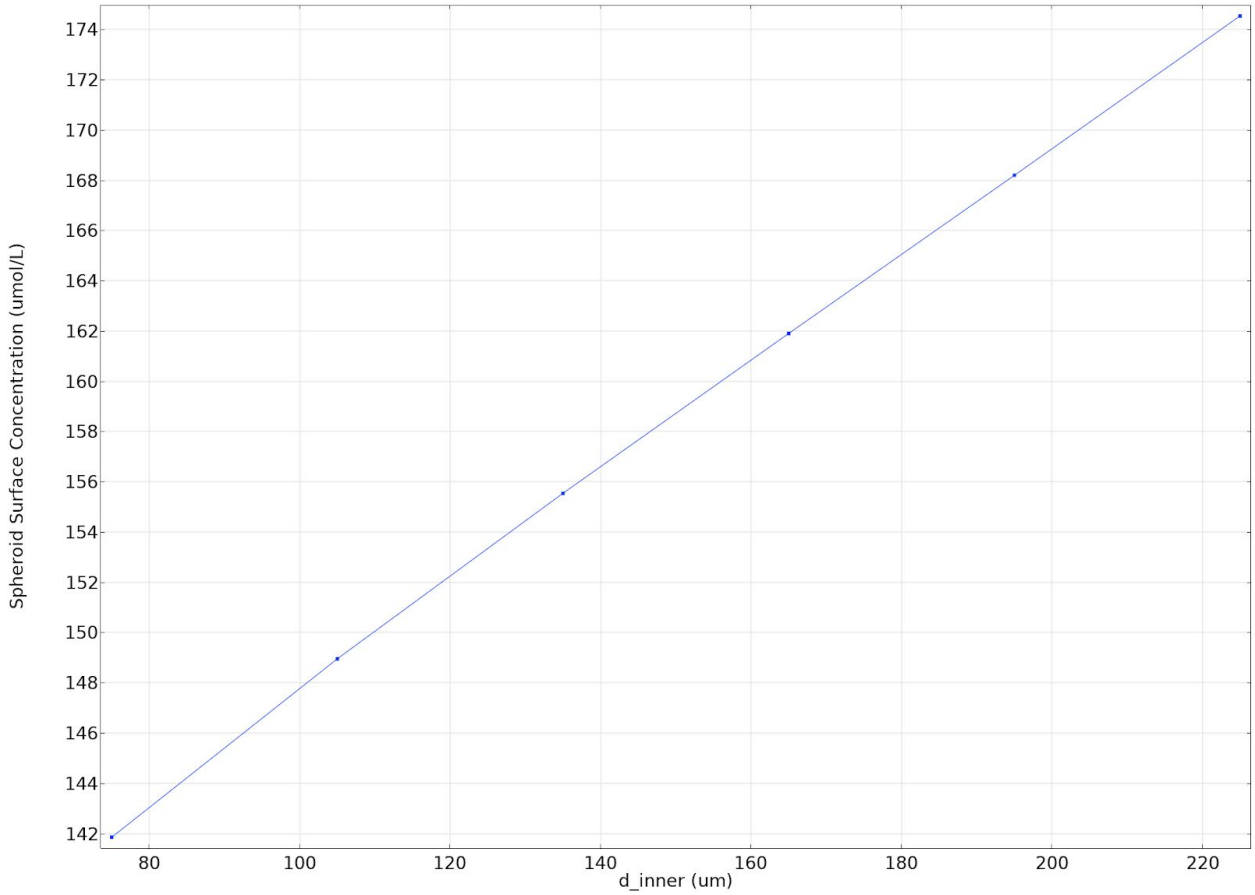

Figure 12: Spheroid surface concentration vs. inner fiber diameter. The variables are directly proportional.

Although not calculated for in the simulations, the membranes also allow other molecules such as nutrients, waste, and even medium to pass in or out, depending on the local gradient. Thus, experimenters should test an array of membrane porosities and thicknesses to obtain the highest values for maximum oxygen delivery while maintaining proper transfer rates of the other components.

Unit Cell Height Sweep

In this sweep, we change the unit cell height (z-axis). At the minimum swept value, the crossed fibers are touching. Execution time for the laminar flow study is 4 min while for the mass transfer study is 29.58 min. **Figure 13** below shows the result for a unit cell height of 750 µm. Note that the crossed fibers do not touch anymore. The spheroid surface concentration is equal to that of the extra-capillary space. In fact, the concentration profile looks nearly the same as the baseline in **Figure 6**.

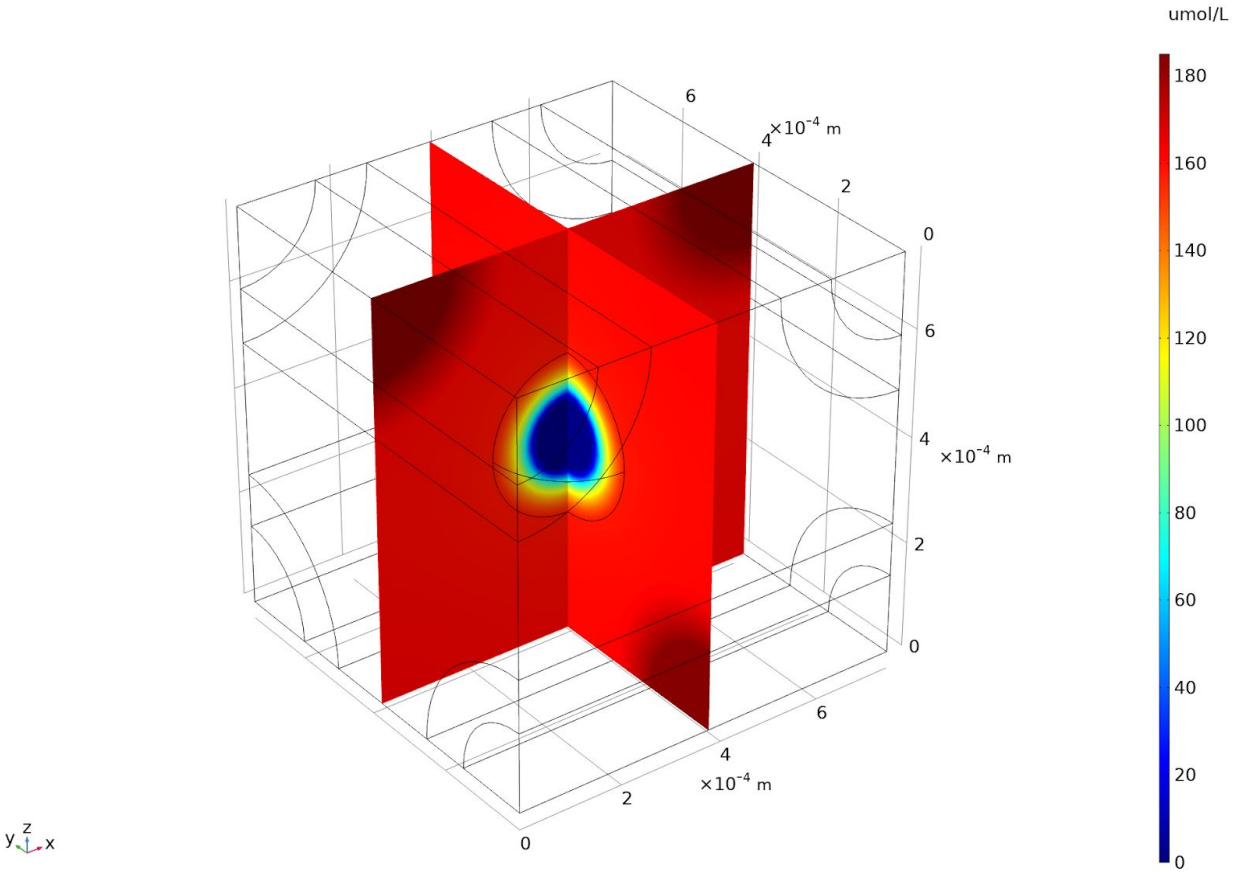

Figure 13: Concentration profile. Unit cell height (z-axis) is 750 μm.

Figure 14 below shows the result of sweeping unit cell height on the spheroid surface concentration. With increasing unit cell height, the surface concentration slightly increases. Surprisingly, this goes against our hypothesis that increasing the unit cell height decreases surface concentration due to the increased distance between the sources (lumens) and the spheroid. However, the gap between the minimum swept value and the maximum swept value is very small. Thus, we conclude that changing the unit cell height does not have a significant influence on the objective.

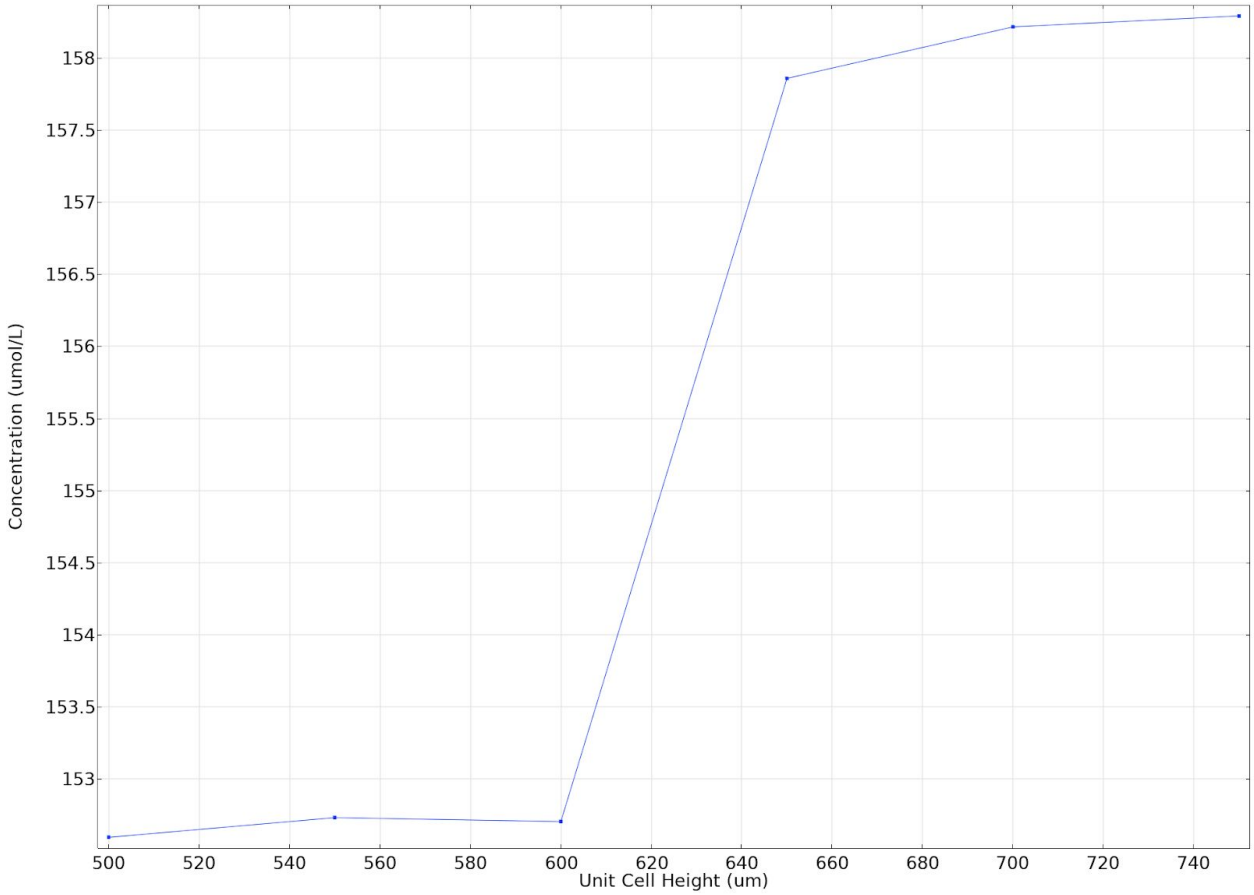

Figure 14: Spheroid surface concentration vs. unit cell height (z-axis).

Conclusion

In this project, we implement the 3D crossed fiber HFMBR model described by Khakpour et al. Simulating a single unit cell within the scaffold with a hepatocyte spheroid situated in the center, we conduct parametric studies on the membrane porosity, membrane thickness, and unit cell height to analyze effects of these parameters on the spheroid surface oxygen concentration, controlled by the laminar flow physics in the lumens and the dilute mass transfer physics in all the domains. This helps in the design of optimized HFMBRs for maximum oxygen delivery to the cells and for reducing the proportion of cells observing a low or zero oxygen concentration. Oxygen is essential for cellular respiration and for maintaining a healthy cell cycle. For in vitro studies, it is often a limiting reactant for cell survival in artificial grafts and bioreactors due to its low solubility. Based on our results, membrane porosity proved to be the most influential parameter. Spheroid surface oxygen concentration greatly decreases as the porosity decreases. In addition, inner fiber diameter, or membrane thickness, also has a great effect on the concentration. Increasing inner diameter causes concentration to increase linearly.

Unit cell height, on the other hand, has trivial effects on the concentration. In short, we recommend a porous, thin membrane for maximum oxygen delivery to the spheroid.

Overall, the HFMBR was found to be capable of delivering a sufficient oxygen supply to the spheroid. Inflowing oxygen with all the fibers allows for a more even concentration profile in the spheroid. In addition, the proportion of cells observing a low or zero concentration is lower than in the paper, where only half the fibers inflow oxygen. For future work, we would simulate the transfer and removal of carbon dioxide from the spheroid to the outlet of the lumens. In addition, modeling the dynamic growth of the spheroid over time and seeing whether the oxygen delivery is actually sufficient would be interesting.

References

[1] Khakpour, S., Renzo, A. D., Curcio, E., Maio, F. P. D., Giorno, L., & Bartolo, L. D. (2017). Oxygen transport in hollow fibre membrane bioreactors for hepatic 3D cell culture: A parametric study. *Journal of Membrane Science*, *544*, 312–322. doi: 10.1016/j.memsci.2017.09.024